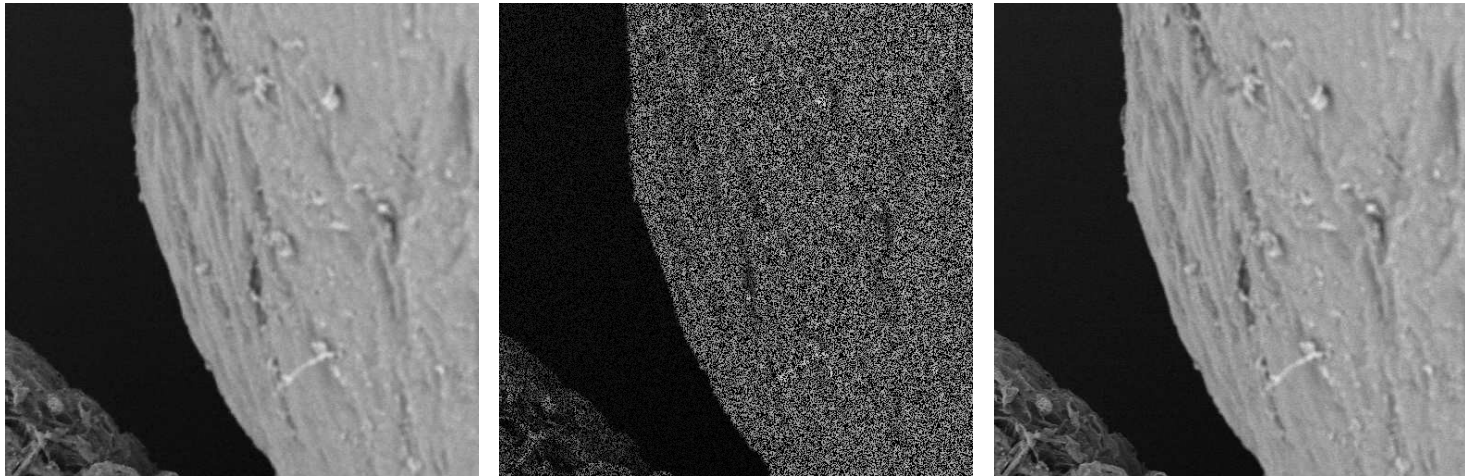


Exceptional service in the national interest



Compressed Sensing for fast electron microscopy

Hyrum Anderson, Jason Wheeler, Kurt Larson
Sandia National Laboratories
Albuquerque, NM



Sandia National Laboratories is a multi-program laboratory managed and operated by Sandia Corporation, a wholly owned subsidiary of Lockheed Martin Corporation, for the U.S. Department of Energy's National Nuclear Security Administration under contract DE-AC04-94AL85000. SAND NO. 2011-XXXX

Outline

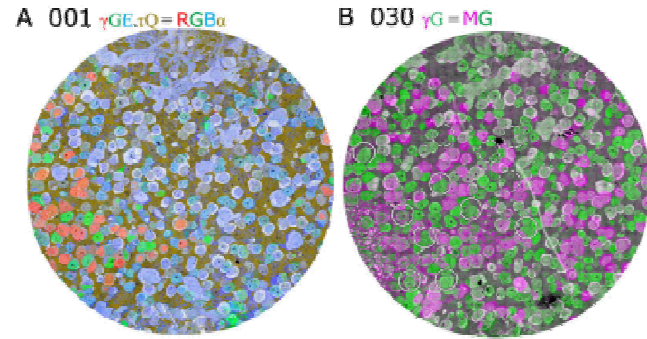
- Background and Motivation
- Previous work: sparse sampling an operational SEM
- Analysis of multi-beam measurements
- Summary

SNR-limited image collection time

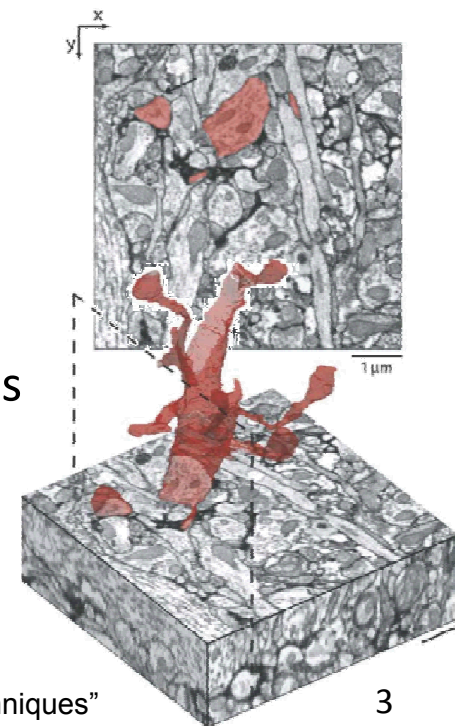
- Rabbit retina connectome (Anderson, et al., 2011)
 - Tissue ~ 0.25 mm in diameter
 - ~ 2 nm resolution
 - 350,000 image tiles (16.5 TB) in 5 months
 - Automated trans. electron microscope
- Mouse brain (Briggman and Denk, 2006)
 - Single cortical column from mouse ~ 0.1 mm 3
 - ~ 10 nm / pixel per 30 nm slice
 - Thousands of images (10^8 pixels each) over several months
 - Serial block-face SEM
- Many engineering efforts to reduce collection time

(Lichtman et al. @ Harvard)

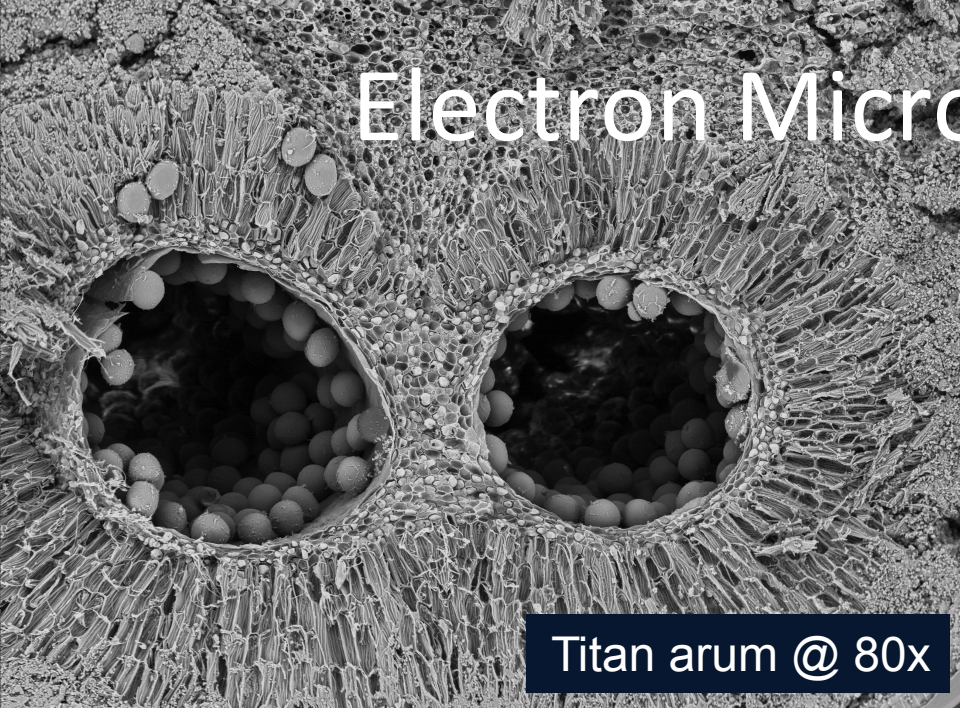
Briggman and Denk, 2006, "Towards neural circuit reconstruction with volume electron microscopy techniques"



Anderson, et al., 2011, "Exploring the retinal connectome"

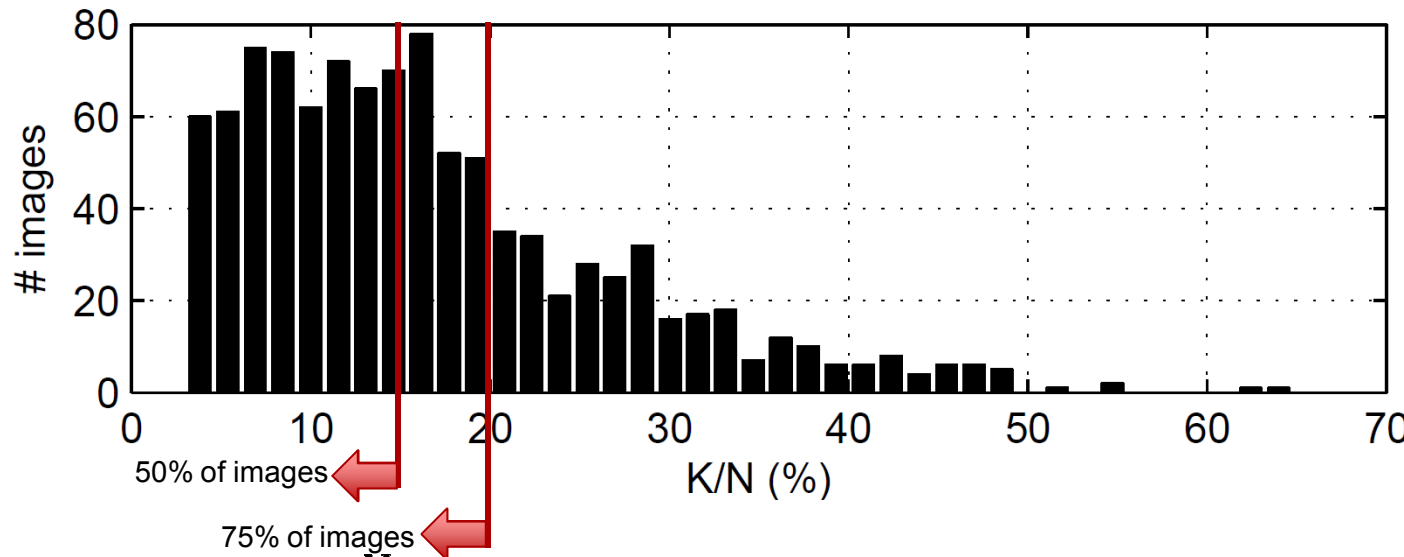


Electron Microscopy Images



SEM Image Compressibility

- Compression basis: block-DCT (similar to JPEG)
- K = # of coefficients required to capture at least 99.75% of image energy
- N = # of image pixels



- $M \geq O(K \log \frac{N}{K})$ # of measurements for recovery by CS

Images courtesy of Dartmouth public domain gallery: <http://www.dartmouth.edu/~emlab/gallery>

Previous Work

- Visit a random subset of pixel locations (Φ a subset of \mathbf{I})
- Measurement model: $\mathbf{y} = \Phi\mathbf{x} + \mathbf{n} \quad E(\mathbf{n}\mathbf{n}^T) = \sigma^2\mathbf{I}$
- From $M < N$ measurements, reconstruct via

$$\begin{aligned} \min_{\mathbf{x}} \quad & \|\Psi^T \mathbf{x}\|_1 + \|\nabla \mathbf{x}\|_1 \\ \text{s.t.} \quad & \|\mathbf{y} - \Phi\mathbf{x}\| \leq \sigma^2 \end{aligned}$$

- Compression basis Ψ chosen to be block-DCT
 - Good compressibility of SEM images
 - Low mutual coherence
- Total variation regularizer $\|\nabla \mathbf{x}\|_1$ to denoise and promote smoothness between block boundaries

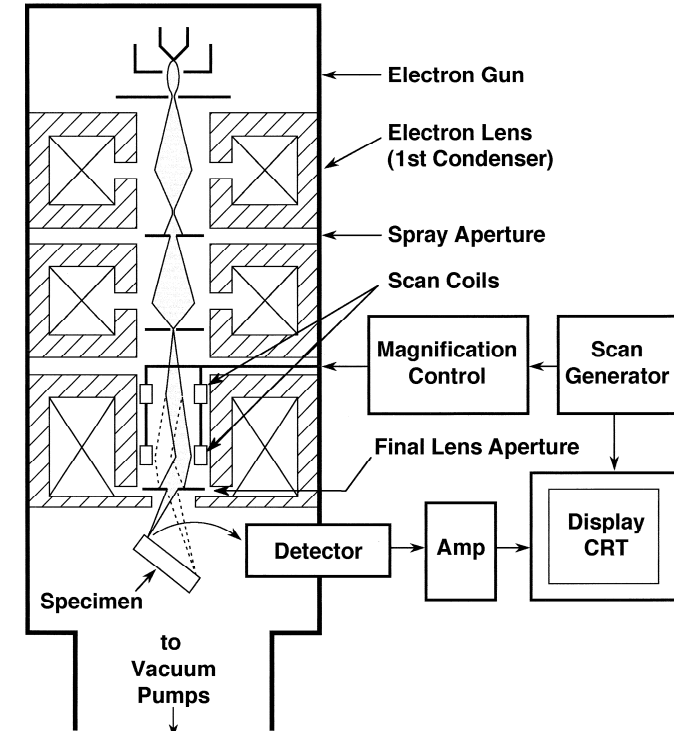
Scan coil dynamics

- Electron probe positioned via electromagnetic coils

$$\mathbf{F} = q [\mathbf{E} + (\mathbf{v} \times \mathbf{B})]$$

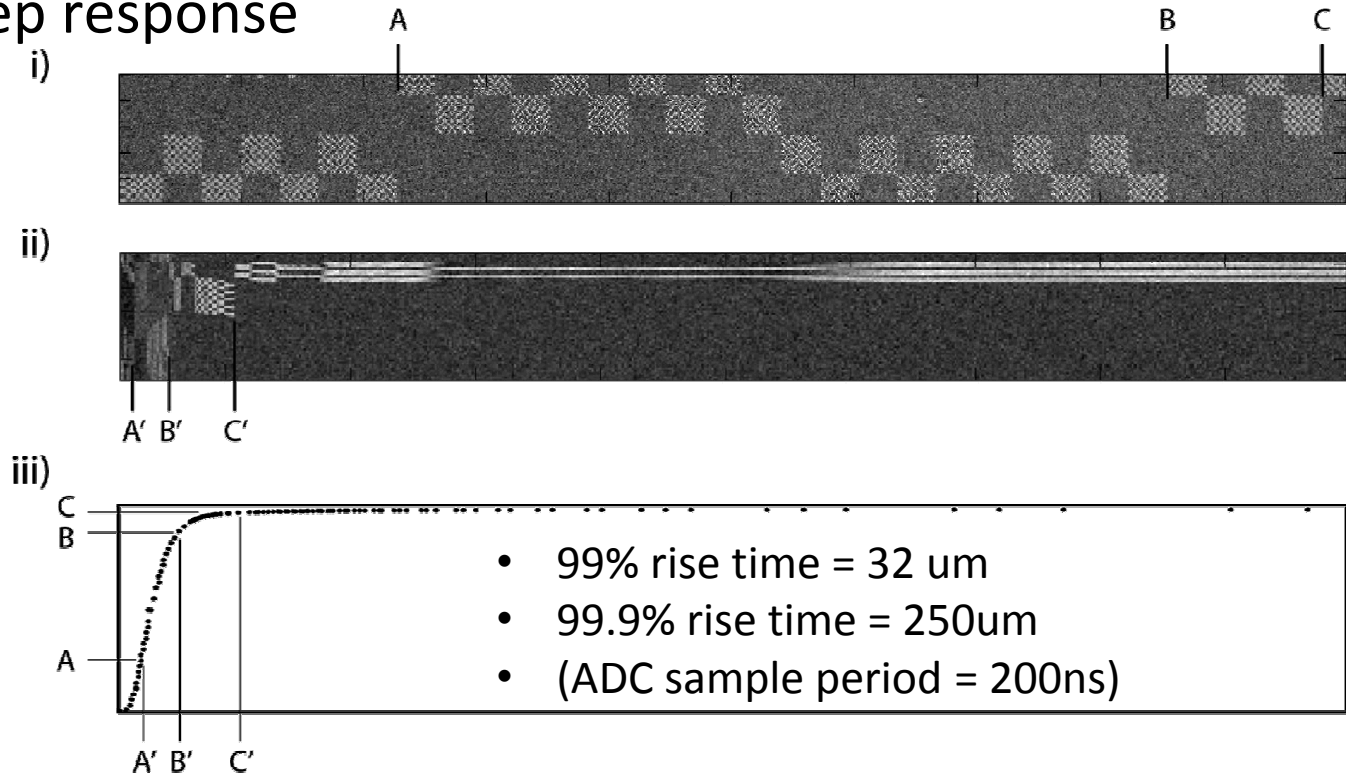
- Slow compared to sample period

- Commanded position \neq actual position
 - Transient delay
 - Steady state lage



Scan coil dynamics

- Measure step response



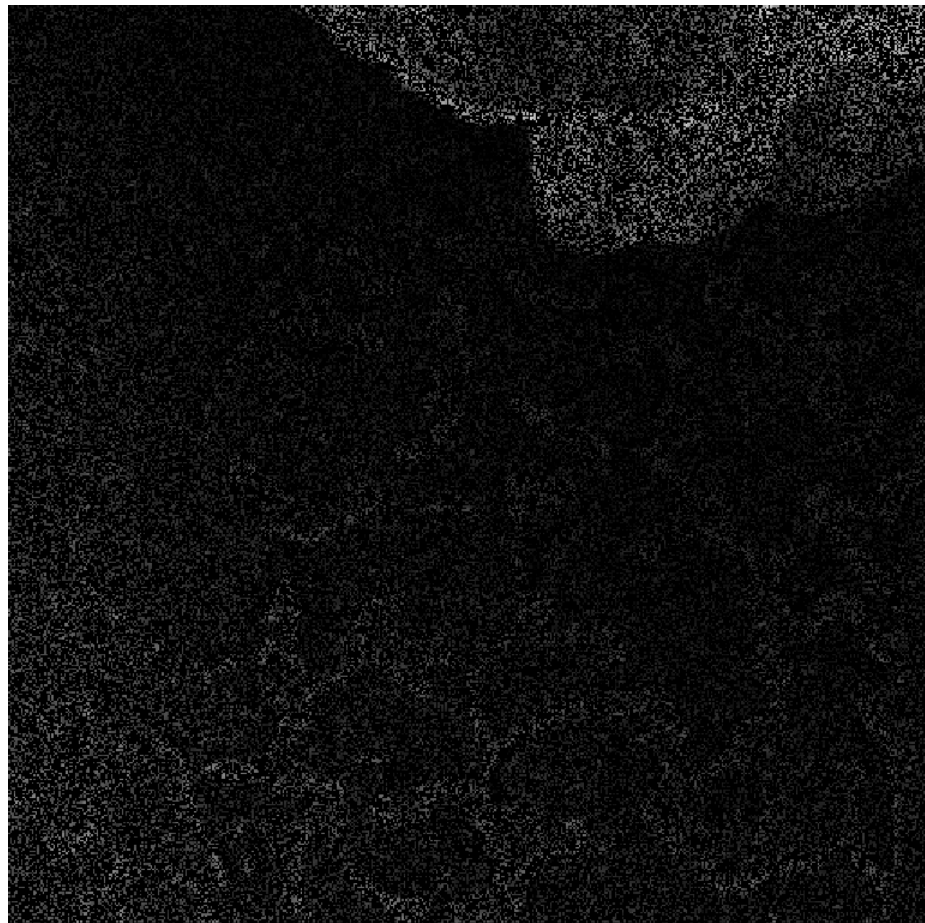
- Linear dynamical model to predict “actual” location

$$\frac{d^5x(t)}{dt^5} = a_0(\hat{x}(t) - x(t)) - a_1 \frac{dx(t)}{dt} - a_2 \frac{d^2x(t)}{dt^2} - a_3 \frac{d^3x(t)}{dt^3} - a_4 \frac{d^4x(t)}{dt^4}$$

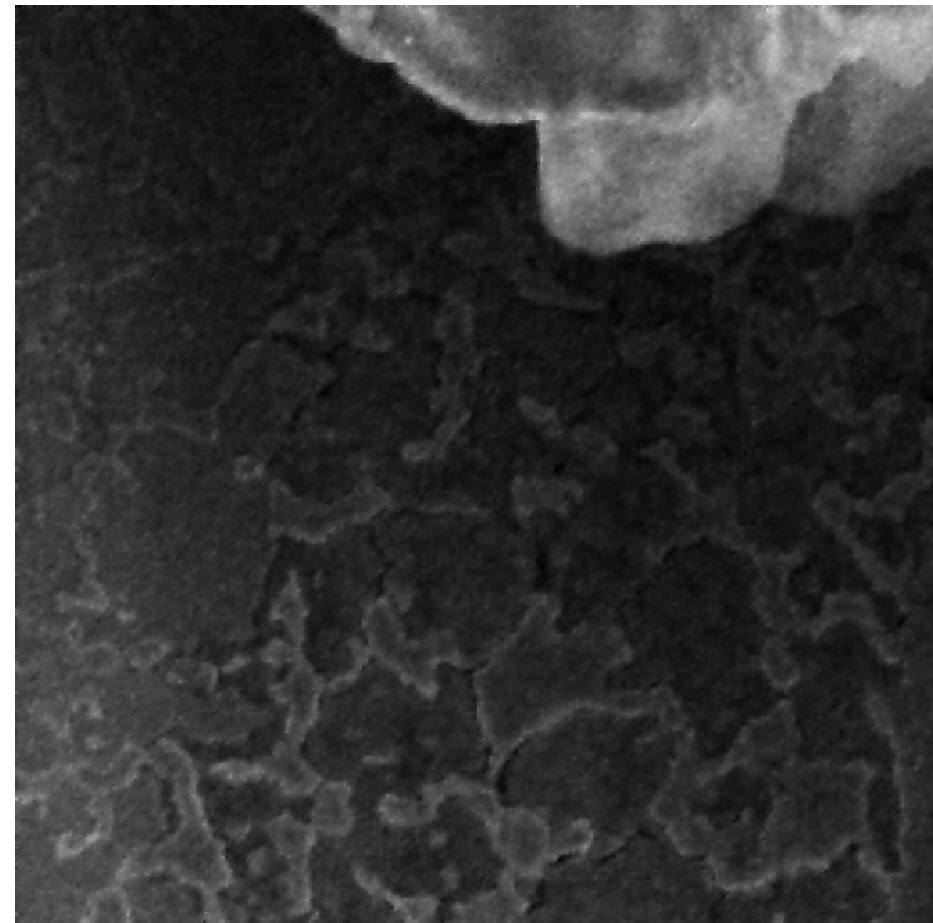
Simulated: Gibeon meteorite surface

(noiseless simulated recover)

M/N = 30%

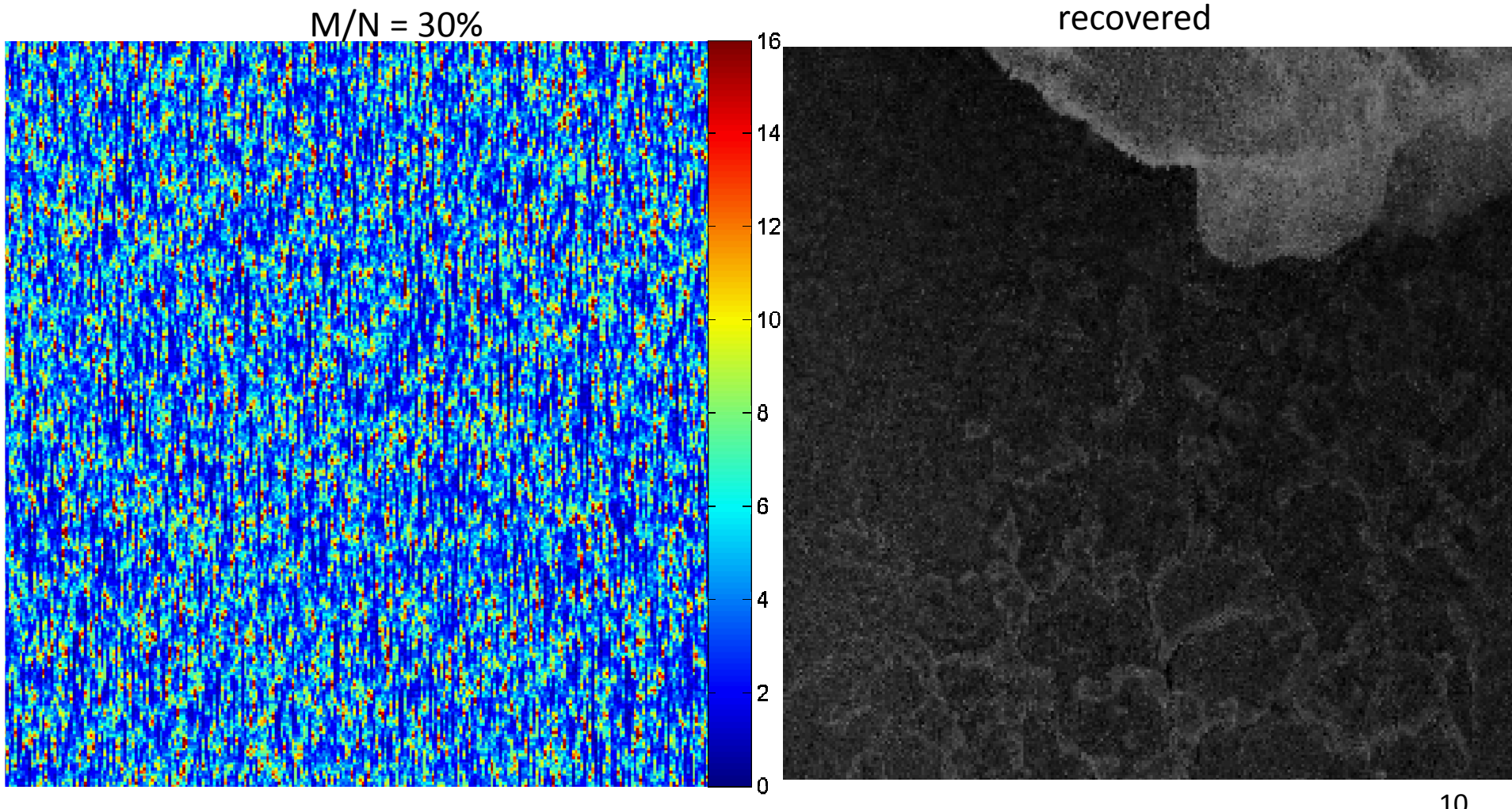


recovered

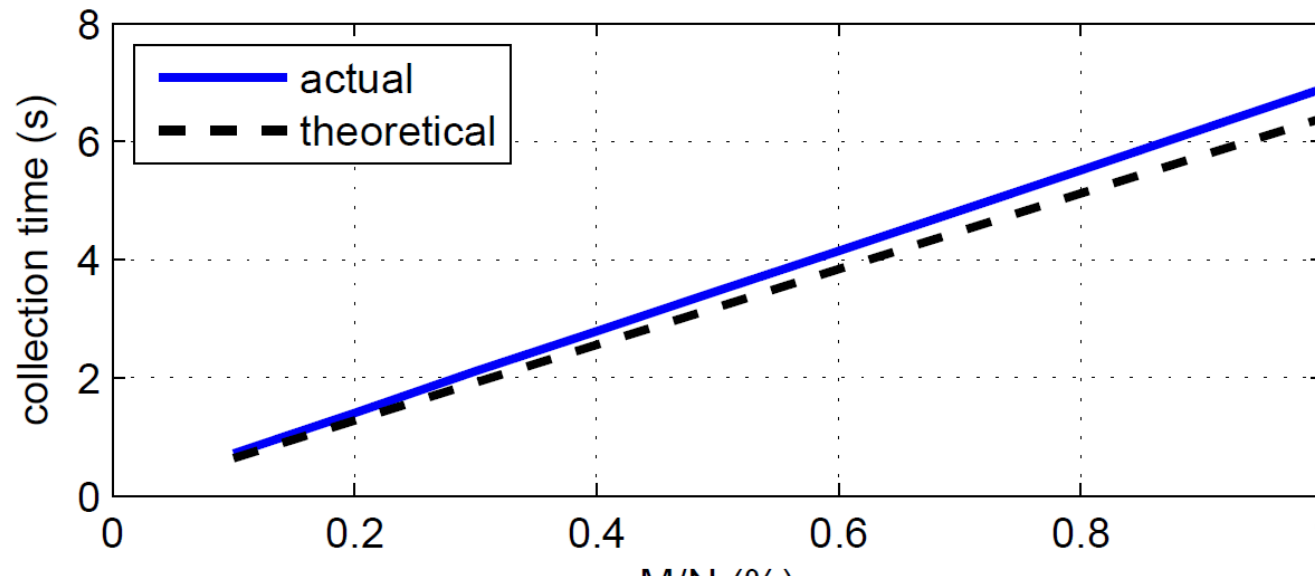


Actual: Gibeon meteorite surface

(actual measurement location + recovery)



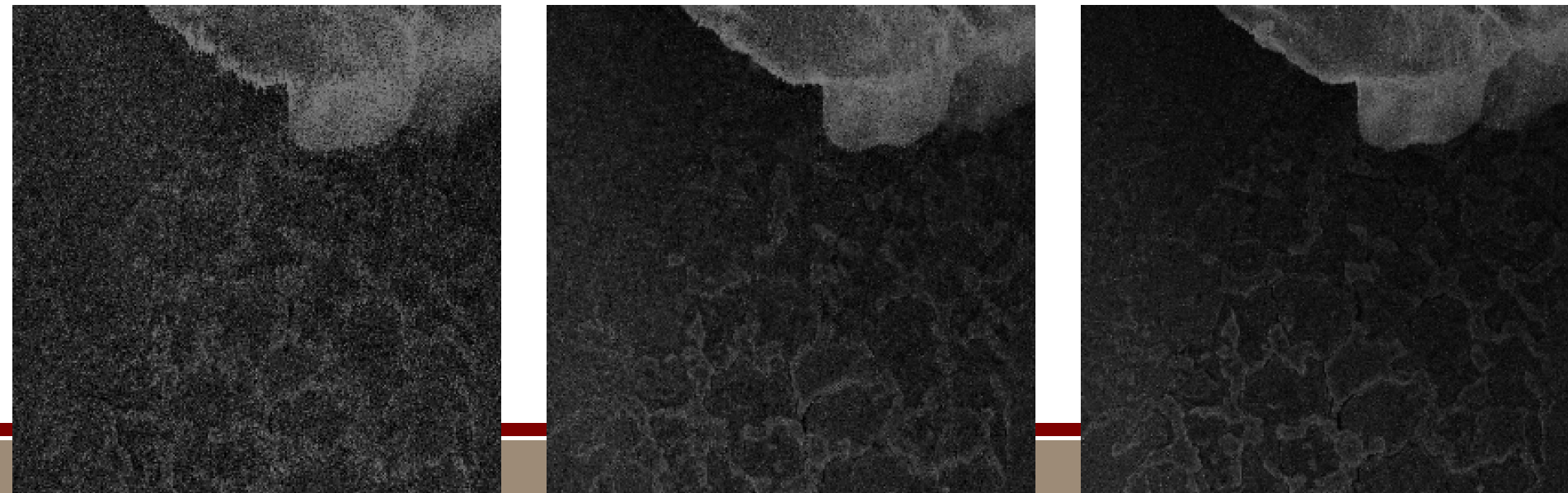
Undersampling timing results



$M/N = 10\%$

$M/N = 30\%$

$M/N = 50\%$



Sparse sampling summary

- Preliminary demonstration of sparse sampling & reconstruction in an operational SEM
- Acceptable image quality at 2-3x speedup
- Speedups **in series** with other engineering advances

Shortcomings:

- Requires $\sim 10x$ more time to reconstruct data than to collect
- Only viable for “smooth” images (compressible by block-DCT)

Outline

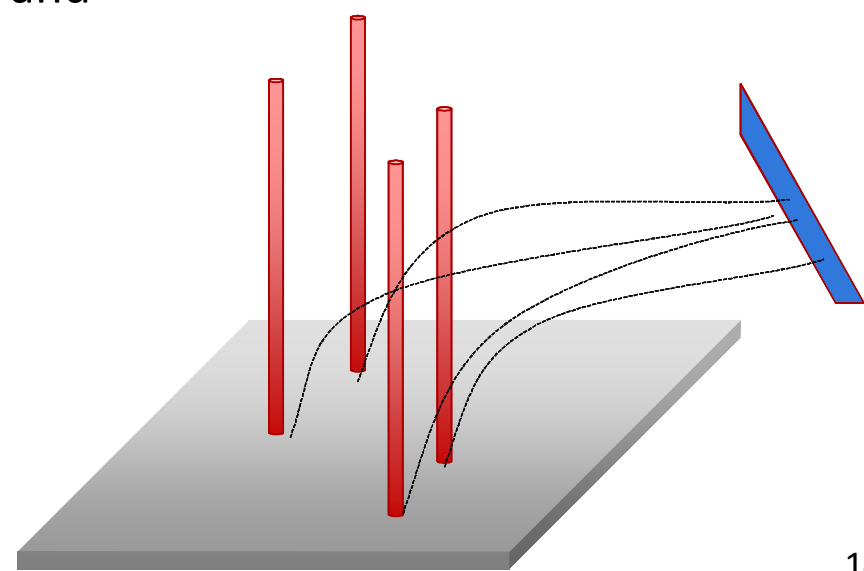
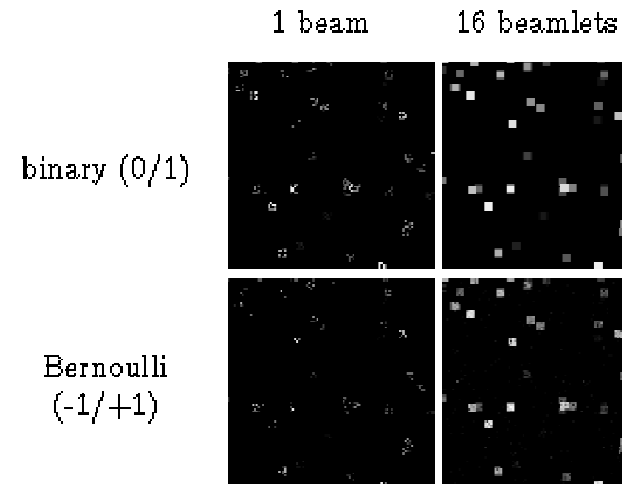
- Background and Motivation
- Previous work: sparse sampling an operational SEM
- Analysis of multi-beam measurements 
- Summary

Multiple beams, single detector

Multiplexed measurements enable reconstructing broader class of images

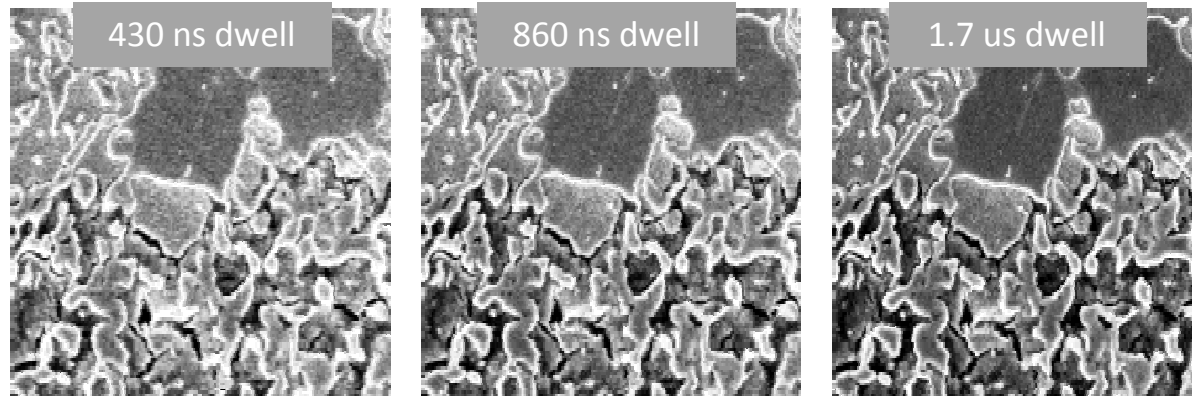
Hypothetical multibeam tool:

- Multi-beam source projects sparse, programmable pattern on the sample
- Single detector with linear response and sufficient dynamic range



Experimental setup

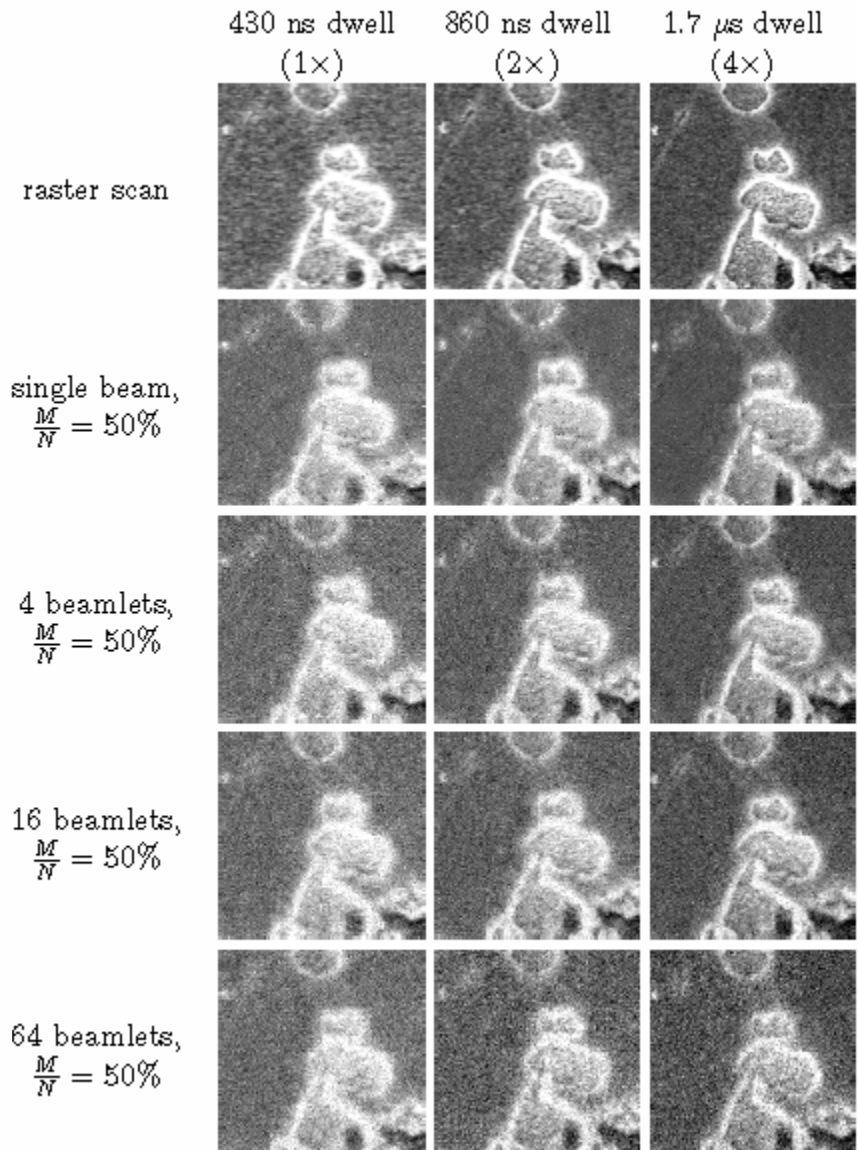
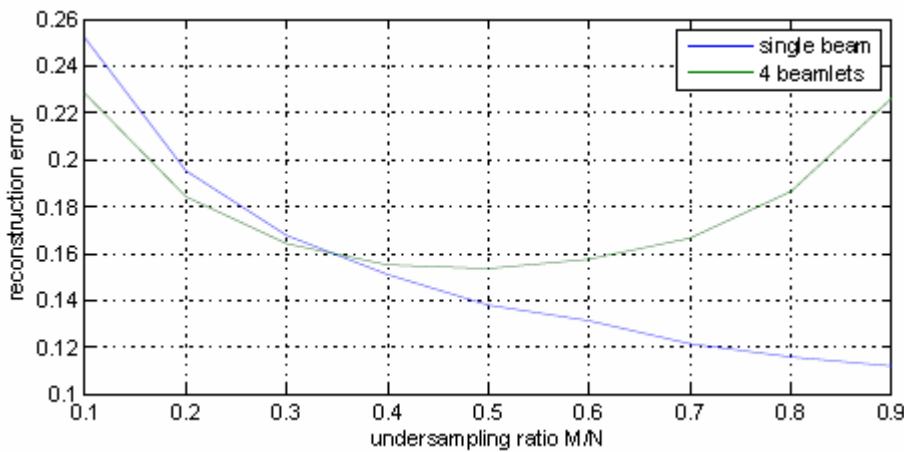
- Commercially available SEM column from Zeiss GmbH
 - Schottky thermal field emission source
 - Nominal beam energy of 10 kEV, 10 um aperture, ~200 pA beam
 - Secondary electron detector
- Collect 1000 800x800-pixel images of single area of interest
 - Register image stack after collection to compensate for drift



- Synthesize multibeam measurements in software
 - Simple sum of responses from selected pixels, adds intensity + noise
 - Assumes (incorrectly) no detector noise

Results

- Using a few beamlets
 - Provides moderate quality improvement over sparse imaging for “large” M/N (50%)



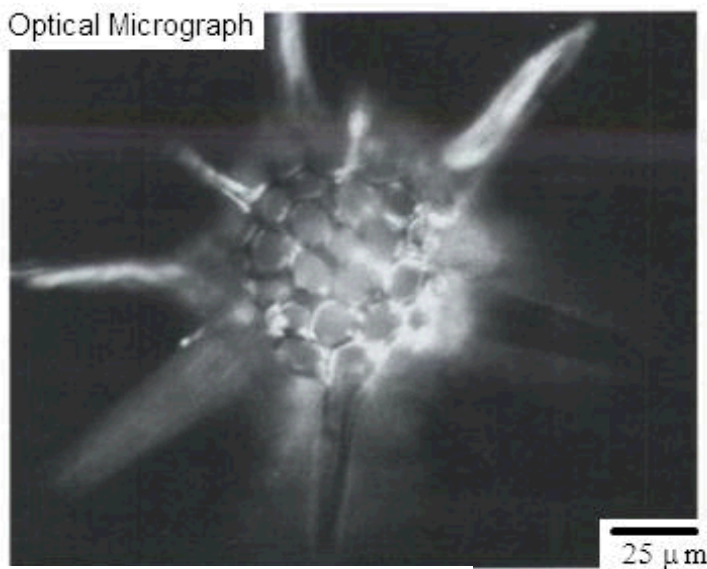
Summary

- **Single-beam sparse sampling:**
 - acceptable image quality at 2-3x speedup
 - speedups **in series** with other engineering advances
 - **demonstrated in operational tool**
 - Doesn't generalize to non-smooth images
- **Multibeam compressed sampling:**
 - Possibly provides modest quality improvement over sparse sampling for speedup of $\sim 2x$ or less
 - Generalizes to non-smooth images
 - Synthetic multibeam measurements lack appropriate noise conditions, optimistic in some settings (linear detector), pessimistic in others (detector noise)

[backup slides]

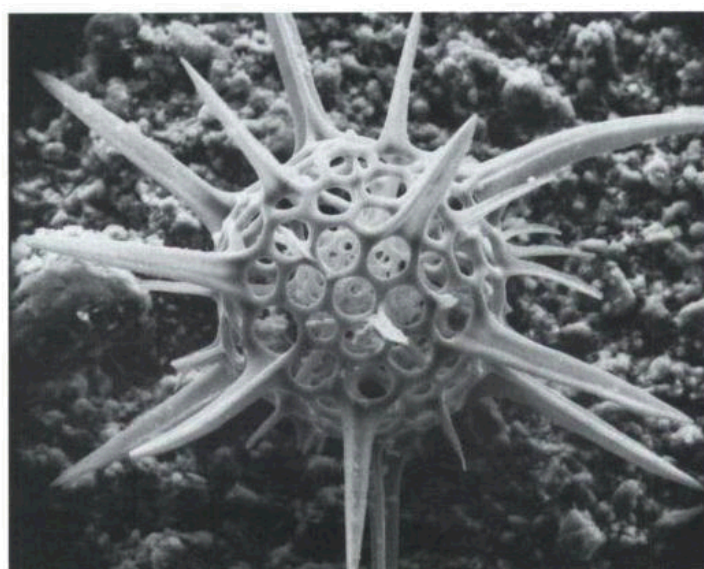
Why SEM?

Optical Microscope Image



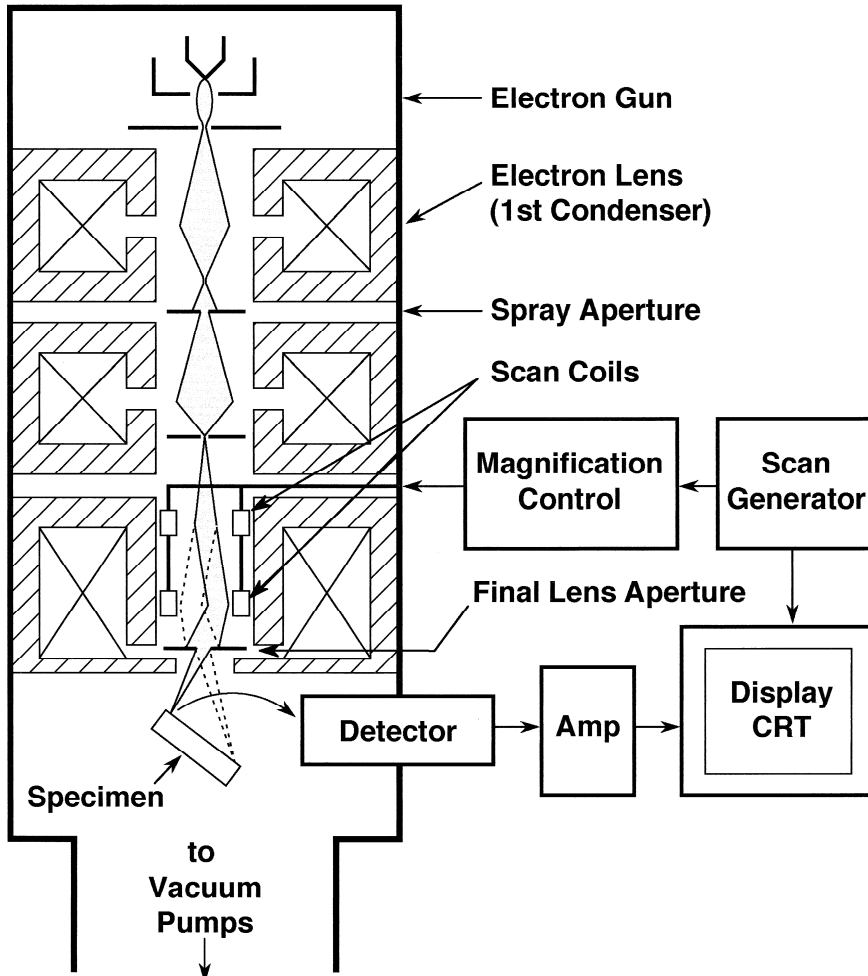
Radiolarian (marine organism)

SEM Image



- Typical SEMs can resolve ~ 1 nm features (10^3 x smaller diff. limit than optical)
- Large depth of focus
- Flexible viewing conditions, e.g., 10x to 500,000x mag

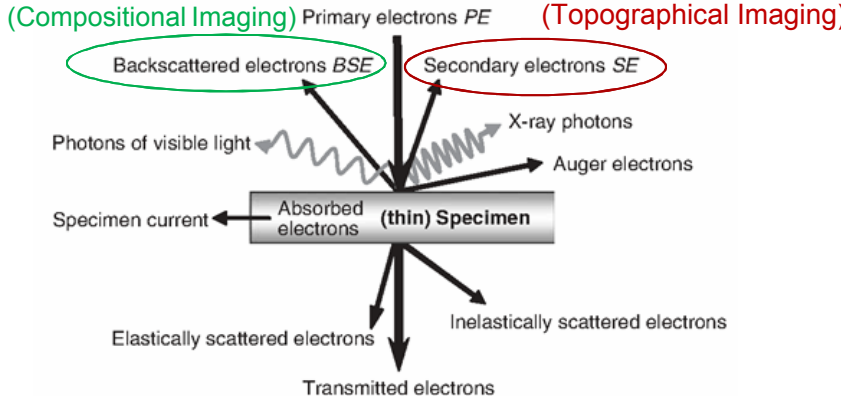
SEM Electron Column



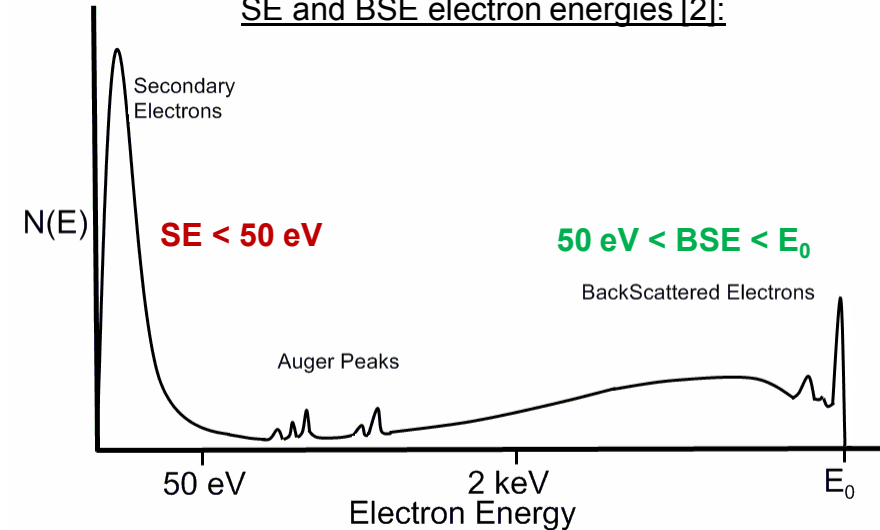
- Electron gun generates electrons
- Electromagnetic condenser lenses and apertures focus electrons into a beam w/ small spot size (~1 nm)
- Scan coils raster beam across sample area to be imaged
- Detector collects electrons at each point of raster pattern and plots on computer display (typically a single SE/BSE, but there may be other, specialized detectors).

Interaction of Electrons with Solids

Probe/sample interactions [1]:



SE and BSE electron energies [2]:



- Electron interaction with a solid results in a number of processes
- SEM uses scattered electrons for sample imaging
- **Backscattered electrons (BSEs):**
 - elastic collisions with atoms nuclei
 - high energy => heavily influenced by atomic number of material (He Z=2, Au Z=79)
- **Secondary electrons (SEs):**
 - weakly bound electrons excited from the sample
 - low energy => heavily influenced by surface topography

[1] D..J. Stokes, *Principles and Practice of Variable Pressure/Environments Scanning Electron Microscopy* (John Wiley & Sons, Ltd., UK, 2008).

[2] From J. Mabon, *SEM and FIB in Materials Research*, UIUC

Collection of Scattered Electrons

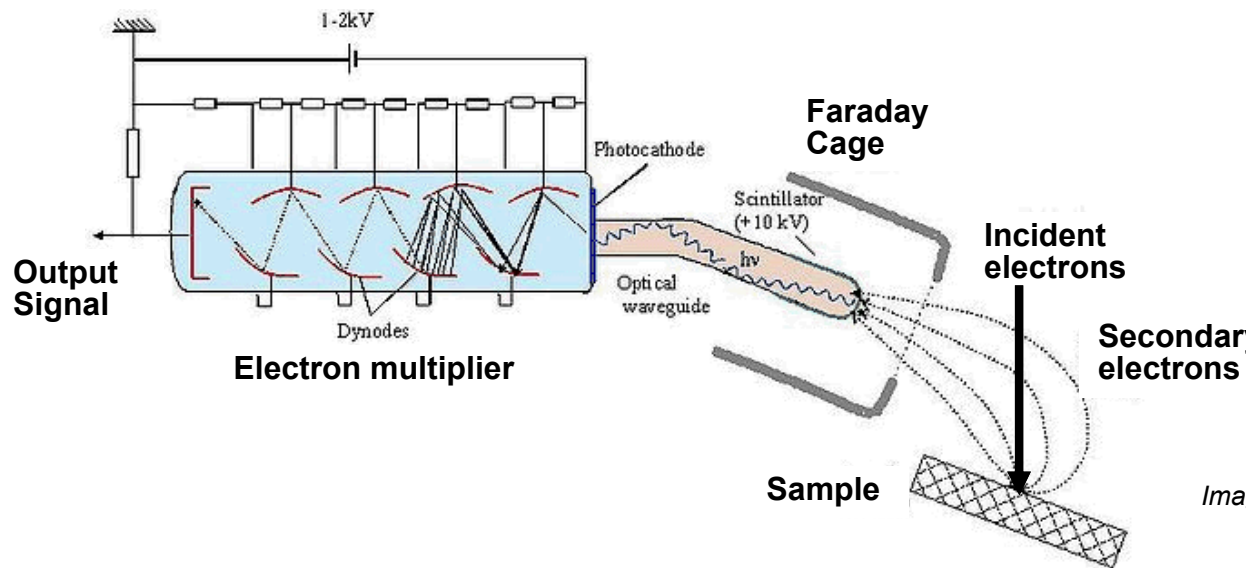
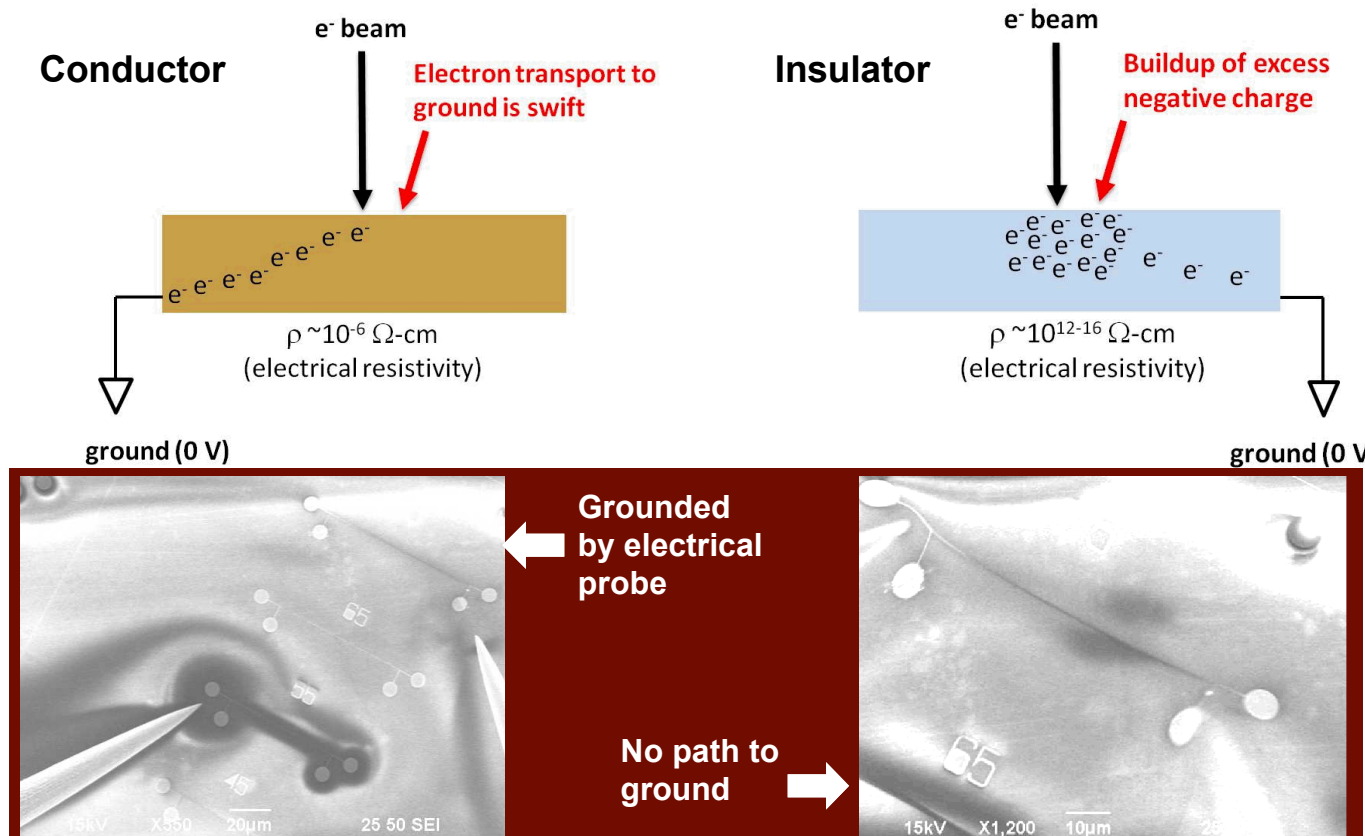


Image courtesy of fr.wikipedia.org

- Everhart-Thornley (E-T) detectors are the most widely used detectors in SEM. Can measure both backscattered electrons (BSE) and secondary electrons (SE).
- Bias voltage on Faraday cage & scintillator selects between BSE and SE. This is small compared to the primary beam (~few hundred V).
- Electron that passes Faraday cage strikes a scintillator, which converts the signal to light that is directed down an optical waveguide
- The light signal is converted back to electrons (at photocathode), which is amplified by an electron multiplier (gain $\sim 10^5$ - 10^6) and collected by software

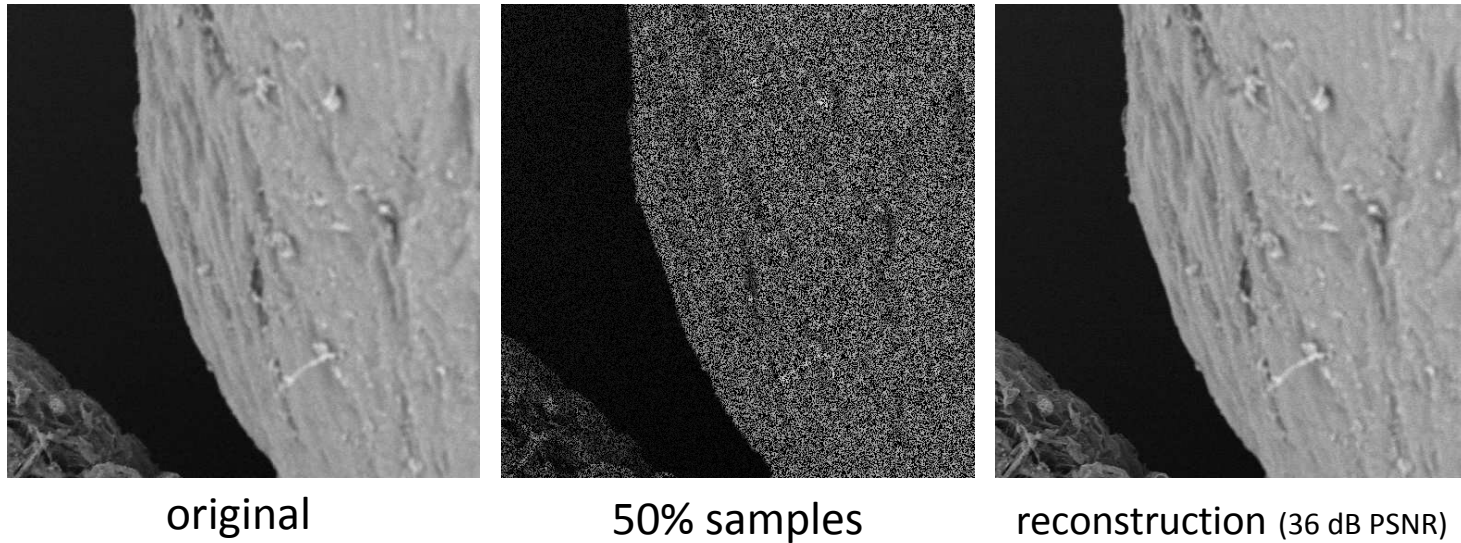
Challenge #2: sample charging

- Charging: electron buildup in sample with no path-to-ground
- Causes image distortion: Surface potential large enough to deflect electrons incident to or reflected from the sample



Sparse reconstruct example

- Interpolation + denoising using block-DCT with TV regularizer



- What about simpler/more efficient bilinear interpolation?
(more efficient, but brittle to noise)

Implementation

- Solve efficiently via split Bregman method (Goldstein & Osher, 2009)

$$(\text{unconstrained}) \quad \min_{\mathbf{x}} \|\Psi^T \mathbf{x}\|_1 + \|\nabla \mathbf{x}\|_1 + \frac{\mu}{2} \|\mathbf{y} - \Phi \mathbf{x}\|_2^2$$

solve for image and auxiliary variables:

$$\begin{aligned} \min_{\mathbf{x}, \mathbf{u}, \mathbf{v}, \mathbf{w}} \quad & \|\mathbf{w}\|_1 + \|(\mathbf{u}, \mathbf{v})\|_2 + \frac{\mu}{2} \|\Phi \mathbf{x} - \mathbf{y}\|_2^2 \\ & + \frac{\lambda}{2} \|\mathbf{u} - \nabla_u \mathbf{x} - \mathbf{b}_u^k\|_2^2 + \frac{\lambda}{2} \|\mathbf{v} - \nabla_v \mathbf{x} - \mathbf{b}_v^k\|_2^2 + \frac{\gamma}{2} \|\mathbf{w} - \Psi^T \mathbf{x} - \mathbf{b}_w^k\|_2^2. \end{aligned}$$

update Bregman parameters

$$\mathbf{b}_u^{k+1} = \mathbf{b}_u^k + (\nabla_u \mathbf{x}^{k+1} - \mathbf{u}^{k+1})$$

$$\mathbf{b}_v^{k+1} = \mathbf{b}_v^k + (\nabla_v \mathbf{x}^{k+1} - \mathbf{v}^{k+1})$$

$$\mathbf{b}_w^{k+1} = \mathbf{b}_w^k + (\Psi^T \mathbf{x}^{k+1} - \mathbf{w}^{k+1})$$

Implementation

$$\begin{aligned}
 \min_{\mathbf{x}, \mathbf{u}, \mathbf{v}, \mathbf{w}} \quad & \|\mathbf{w}\|_1 + \|(\mathbf{u}, \mathbf{v})\|_2 + \frac{\mu}{2} \|\Phi \mathbf{x} - \mathbf{y}\|_2^2 \\
 & + \frac{\lambda}{2} \|\mathbf{u} - \nabla_u \mathbf{x} - \mathbf{b}_u^k\|_2^2 + \frac{\lambda}{2} \|\mathbf{v} - \nabla_v \mathbf{x} - \mathbf{b}_v^k\|_2^2 + \frac{\gamma}{2} \|\mathbf{w} - \Psi^T \mathbf{x} - \mathbf{b}_w^k\|_2^2
 \end{aligned}$$

- Alternating minimizations
 - Efficient solution for $\mathbf{w}, \mathbf{u}, \mathbf{v}$ via elementwise shrinkage
 - Efficient (inexact) solution to \mathbf{x} via Fourier (circulant approx)

diagonal
 (non-constant) circulant

$$\begin{aligned}
 & (\mu \Phi^T \Phi - \lambda \Delta + \gamma \mathbf{I}) \mathbf{x} = \\
 & \quad \mu \Phi^T \mathbf{y} + \lambda \nabla_u^T (\mathbf{u}^k - \mathbf{b}_u) + \lambda \nabla_v^T (\mathbf{v}^k - \mathbf{b}_v) + \gamma \Psi (\mathbf{w}^k - \mathbf{b}_w)
 \end{aligned}$$

Phase transition curves

